

Article

User-Friendly Reverse Genetics System for Modification of the Right End of Fowl Adenovirus 4 Genome

Bingyu Yan ^{1,2}, Xiaohui Zou ², Xinglong Liu ^{1,2}, Jiaming Zhao ^{2,3}, Wenfeng Zhang ^{2,3}, Xiaojuan Guo ², Min Wang ², Yingtao Lv ^{1,*} and Zhuozhuang Lu ^{2,4,5,*}

¹ College of Marine Science and Biological Engineering, Qingdao University of Science and Technology, Qingdao 266042, China; yanbingyusd@163.com (B.Y.); lxlsddz01@163.com (X.L.)

² State Key Laboratory of Infectious Disease Prevention and Control, National Institute for Viral Disease Control and Prevention, Chinese Center for Disease Control and Prevention, Beijing 100052, China; zouxh@ivdc.chinacdc.cn (X.Z.); zhaojm777@163.com (J.Z.); zhangwfme@163.com (W.Z.); guoxj@ivdc.chinacdc.cn (X.G.); wangmin@ivdc.chinacdc.cn (M.W.)

³ Department of Laboratory Medicine, School of Public Health and Management, Weifang Medical University, Weifang 261053, China

⁴ Center for Biosafety Mega-Science, Chinese Academy of Sciences, Wuhan 430071, China

⁵ Chinese Center for Disease Control and Prevention-Wuhan Institute of Virology, Chinese Academy of Sciences Joint Research Center for Emerging Infectious Diseases and Biosafety, Wuhan 430071, China

* Correspondence: luzz@ivdc.chinacdc.cn (Z.L.); lvyingtao@qust.edu.cn (Y.L.); Tel.: +8610-63511368 (Z.L.)

Received: 7 February 2020; Accepted: 9 March 2020; Published: 11 March 2020



Abstract: A novel fowl adenovirus 4 (FAdV-4) has caused significant economic losses to the poultry industry in China since 2015. We established an easy-to-use reverse genetics system for modification of the whole right and partial left ends of the novel FAdV-4 genome, which worked through cell-free reactions of restriction digestion and Gibson assembly. Three recombinant viruses were constructed to test the assumption that species-specific viral genes of ORF4 and ORF19A might be responsible for the enhanced virulence: viral genes of ORF1, ORF1b and ORF2 were replaced with GFP to generate FAdV4-GFP, ORF4 was replaced with mCherry in FAdV4-GFP to generate FAdV4-GX4C, and ORF19A was deleted in FAdV4-GFP to generate FAdV4-CX19A. Deletion of ORF4 made FAdV4-GX4C form smaller plaques while ORF19A deletion made FAdV4-CX19A form larger ones on chicken LMH cells. Coding sequence (CDS) replacement with reporter mCherry demonstrated that ORF4 had a weak promoter. Survival analysis showed that FAdV4-CX19A-infected chicken embryos survived one more day than FAdV4-GFP- or FAdV4-GX4C-infected ones. The results illustrated that ORF4 and ORF19A were non-essential genes for FAdV-4 replication although deletion of either gene influenced virus growth. This work would help function study of genes on the right end of FAdV-4 genome and facilitate development of attenuated vaccines.

Keywords: fowl adenovirus; reverse genetics system; Gibson assembly; restriction enzyme; essential gene

1. Introduction

Fowl adenoviruses (FAdV) belong to the family of Adenoviridae and the genus of *Aviadenovirus* [1]. Currently 12 types of FAdV have been identified (FAdV-1 to -8a and -8b to 11), which are further classified into five species (*FAdV-A to -E*) [2]. FAdVs are believed to be the pathogens causing adenoviral gizzard erosion (AGE), inclusion body hepatitis (IBH) and hepatitis-hydropericardium syndrome (HHS) in chickens, although the outcome of an FAdV infection depends on many factors including

serotype and strain of the virus, type and age of the host, and the route of inoculation [3]. FAdV-4 is the predominant causative agent of HHS, which is characterized by an accumulation of clear, straw-colored fluid in the pericardial sac and a swollen, friable, discolored liver with focal necroses and petechial hemorrhages. The first outbreak of FAdV-4 occurred near Karachi, Pakistan in 1987 [4]. After that, the virus has spread to most of Asia, Central and South America, and some European countries. Since July 2015, outbreaks of HHS caused by a novel genotype of FAdV-4 have been reported in China, causing significant economic losses to the poultry industry [5–7].

The family of Adenoviridae is composed of five genera, among which the Mastadenovirus, especially human adenovirus species C (HAdV-C), is extensively studied. The adenoviral genes are artificially classified into two groups: the genus-common genes, which are located in the central genome and reserved in all genera, encode structure, replication and encapsidation proteins; and genus-specific genes, which are found at both ends of the viral genome, encode non-structural proteins and play important roles in virus–host interaction [2,8]. Generally, genus-common genes are essential for virus replication in vivo or in vitro cell culture. The function of these genes should be conserved among the family and then be analogous to that of Mastadenovirus. Although most of the genus-specific genes in HAdV-C have been studied, very few genus-specific genes in FAdV have been elucidated in their functions. The reverse genetics system is a valuable approach to study viral genes of FAdV, and some systems have been established and used to construct gene transfer vectors and vectored vaccines [9,10]. Most of these systems work through homologous recombination, which needs the activity of intracellular recombinase.

Here, we attempted to establish a reverse genetics system for the novel strain of FAdV-4 isolated from recent outbreak in China, which was different from existing ones and could be easily applied with our recently introduced technique of restriction-assembly [11,12]. We also characterized some genus-specific genes of FAdV-4 by using this system.

2. Materials and Methods

2.1. Cells, Plasmids and Oligonucleotides

Chicken hepatoma cells (Leghorn Male Hepatoma, LMH) were purchased from American Type Culture Collection (ATCC CRL-2117, Manassas, VA, USA) and were maintained in Dulbecco's modified Eagle's medium (DMEM) plus 10% fetal bovine serum (FBS; HyClone, Logan, UT, USA) at 37 °C in a humidified atmosphere supplemented with 5% CO₂, and passaged twice a week. Flasks or plates were precoated with 0.1% gelatin to help LMH cells spread evenly according to the instructions of ATCC. Plasmid pKFAV4 (plasmid bearing Kanamycin-resistant gene and FAdV-4 genome) was constructed in the laboratory previously [13], which contained the complete genome of the novel FAdV-4 (Genbank accession No. MG547384). pAd5GFP was an E1/E3-deleted HAdV-5-based adenoviral plasmid constructed previously in the laboratory [14], which contained an Enhanced Green Fluorescent Protein (GFP) expression cassette controlled by the human cytomegalovirus (CMV) promoter and SV40 polyA signal.

Plasmid transformation was performed on *Escherichia coli* TOP10 chemically competent cells with the standard heat shock procedure according to the manufacturer's instructions (TIANGEN Biotech, Beijing, China).

For virus rescue or amplification, confluent LMH cells were split at a ratio of 1:3. When the cells had reached 90% confluence, transfection or infection was carried out. After incubation for indicated time, the culture medium was replaced with fresh DMEM containing 2% FBS.

Single-stranded DNA oligos were chemically synthesized. They were used as the primers for Polymerase Chain Reaction (PCR) or used to assemble short double stranded DNA through overlap extension PCR. Information related to these oligos was summarized in Table 1.

Table 1. Summary information of oligonucleotides.

Fragment	Oligo Name	Sequence	Template	Product Length (bp)
AvrII-PacI	1707Avr-PacF	cgaatacagagttggcctaggctctcgacagaacaggggaatggggcattaattaaccgct	self-anneal	96
	1707Avr-PacR	tgctgacttcagccctaggccattggcggagaccgtaagcggttaattaatgcccca		
AgeI-ORF1	1707KFAV4AgeIF	attctccactgctttgaacca	pKFAV4AP	204
	1707KFAV4AgeIR	cccgttaattgattactattacctgtagaaaaagagagaaaattg		
GFP cassette	1707F02GFPF	tttacaaggtaatagtaataacggtcattagtt	pAd5GFP	1672
	1707F02GFPR	tcgatttactgtgaagctacaagtgctagtaagatacattgatgagtttgacaaac		
PvuI-ORF4	1711FAV4GCX5	ggaaccgatcgaagaagcaacag	pKFAV4-GFP	424
	1711FAV4GCX6	gcccttgctcaccatgtcagaatataagagaaggaatgggc		
mCherry CDS	1711FAV4GCX7	ctctatattctgacatggtgagcaaggcgaggag	pmCherry-N1	742
	1711FAV4GCX8	ctggaatagtggttactgtacagctcgtccatgccg		
ORF4-BamHI	1711FAV4GCX9	ggacgagctgtacaagtaacactatattccagtcaggagg	pKFAV4-GFP	180
	1711FAV4GCX10	taagtggatccgcacaccattgc		1281
117-bp linker	1812FAV4APf	cgaaccagtaggcgaatacagagttggcct	pKFAV4AP	117
	1812FAV4APxAr	gggtattagtgtcgtacttcagcccAaggccattggcggagacc		
116-bp linker	1812FAV4SAP1	ccagtaggcgaatacagagttggcctaggctctcgagaacagg	self-anneal	116
	1812FAV4SAP2	tatctctatgctttgTTAATTAAccattccctgttctcgagagcctag g		
	1812FAV4SAP3	aatgggTTAATTAACAaagcatagagataaaagaaacccgttactagtccagga		
	1812FAV4SAP4	ggatttaggaaaagtgttctggactagtaacgggtttctt		
SpeI-BstZ17I	1902FAdV4Xorf19a1	caaagcatagagataaaagaaacccgttac ta	pKFAV4AP	804
	1902FAdV4Xorf19a2	tacaacatttcagtagtttctggtatacattgatgtgaccttcattggcgaac		
CMVp	1904FAV4MCHE1	tcaagtgtatcatatgcccaagtacg	pKFAV4-GFP	395
	1904FAV4MCHE2	ccttgctcaccatggtaggcctctagcggatctgacggttact		
mCherry CDS	1904FAV4MCHE3	ctagaggcctaccatggtgagcaaggcgagga	pmCherry-N1	733
	1904FAV4MCHE4	ggcgtcgactactgtacagctcgtccatgc		1102
mCherry	1906mCHEF1	ggccatcatcaaggagttcatg		623
	1906mCHER1	gttccacgatggtgtagtctctcg		
GFP	1906GFPf	cggccacaagttcagcgtgt c		576
	1906GFPPr	cgcttctcgttggggtctt g		
ORF2	1905ORF2f	ggcttcggaccgttactggg		604
	1905ORF2r	gggggtacggttaatctccc		
ORF19A/ORF4	1905ORF19Af	ctcccgttcaaagtagtgaa ca		737
	1906ORF4r	ggcagatacagcacttcgcagta		

2.2. Construct Intermediate Plasmid pKFAV4AP

Plasmid pKFAV4 (46.2 kb) contained two AvrII sites. Two single-stranded oligonucleotides surrounding the AvrII sites in pKFAV4 were synthesized (Table 1) and fused to form a double stranded DNA (AvrII-PacI, 96 bp in length) through DNA polymerase-mediated extension reaction (Q5 High-Fidelity DNA Polymerase, Cat. M0491S; New England Biolabs, Ipswich, Massachusetts, USA), and a PacI site (ttaattaa) was added in the middle to demarcate the two AvrII-centered parts. pKFAV4 was digested with AvrII, the small fragment (16.7 kb) was recovered from agarose gel (Zymoclean Large Fragment DNA Recovery Kit, Cat.D4045; Zymo Research, Irvine, CA, USA) and mixed with AvrII-PacI fragment, and Gibson assembly was performed to generate an intermediate plasmid pKFAV4AP (pKFAV4 AvrII-PacI) (NEBuilderHiFi DNA Assembly Master Mix, Cat. E2621; New England Biolabs).

2.3. Delete ORF1-ORF2 in pKFAV4

pKFAV4AP was digested with AgeI/NheI, and the fragment of 4942 bp was recovered; PCR was performed to amplify AgeI-ORF1 fragment (Open Reading Frame, ORF; from upstream of AgeI site in ORF0 to ORF1; 204 bp) with primers of 1707KFAV4AgeI/R (Table 1) using pKFAV4AP as the template (Q5 High-Fidelity DNA Polymerase); PCR was performed to amplify GFP expression cassette (1672 bp) with primers of 1707F02GFP/R using pAd5GFP as the template; and these three fragments were fused together to generate plasmid pKFAV4APN-GFP (pKFAV4AP NheI-GFP) by DNA assembly. pKFAV4APN-GFP was digested with NheI, treated with CIP (Calf Intestinal Alkaline Phosphatase; New England Biolabs), and ligated with the large fragment of NheI-digested pKFAV4AP (9840 bp) to generate plasmid pKFAV4AP-GFP (16,575 bp). pKFAV4AP-GFP was digested with PacI and fused to the large fragment of AvrII-digested pKFAV4 (29,468 bp) to generate pKFAV4-GFP (45,981 bp) by DNA assembly (NEBuilderHiFi DNA Assembly Master Mix).

2.4. Replace Coding Sequence of FAdV-4 ORF4 with That of mCherry in pKFAV4-GFP

PvuI and BamHI were single cutters flanking ORF4 coding sequence (CDS) in pKFAV4APN-GFP. A fragment from the PvuI site to the start codon of ORF4, mCherry CDS and a fragment from the stop codon of ORF4 to the BamHI site were amplified by PCR, respectively (primers 1711FAV4GCX5-10, Table 1); and these three fragments were fused together by overlap extension PCR (1281 bp). The 1281-bp fragment was digested with PvuI/BamHI and used to replace the corresponding fragment in pKFAV4APN-GFP to generate pKFAV4APN-GX4C (pKFAV4APN GFP- χ ORF4-mCherry, 6948 bp) through restriction-ligation cloning. pKFAV4APN-GX4C was digested with NheI, treated with CIP and restored to pKFAV4AP to generate pKFAV4AP-GX4C through restriction-ligation cloning. pKFAV4AP-GX4C was digested with PacI and fused to the large fragment of AvrII-digested pKFAV4 to generate pKFAV4-GX4C (46,194 bp) through DNA assembly.

2.5. Remove the AvrII Site in Fiber-2 Gene in pKFAV4 and Reduce the Size of the Intermediate Plasmid

PCR was performed to amplify a 117-bp linker with primers of 1812FAV4APf and 1812FAV4APxAr using pKFAV4AP as the template. pKFAV4AP was digested with AvrII to recover the 16,728 bp fragment, which was fused to the 117-bp PCR product to generate plasmid pKFAV4APX (pKFAV4APxAvrII) through DNA assembly. pKFAV4APX was digested with PacI and fused to the large fragment of AvrII-digested pKFAV4 to generate pKFAV4M (pKFAV4AvrII site-Mutated, 46,196 bp) through DNA assembly.

Overlap extension PCR was employed to generate a 116-bp linker by mixing four primers of 1812FAV4SAP1-4 (Table 1). pKFAV4AP-GFP was digested with AvrII/SpeI, and the fragment of 9476 bp in length was recovered from agarose gel and fused to the 116-bp fragment to generate pKFAV4SAP-GFP (pKFAV4 SpeI-AvrII-PacI GFP, 9540 bp) through DNA assembly.

2.6. Delete ORF19A in pKFAV4-GFP

PCR was performed to amplify an 804 bp fragment with primers of 1902FAdV4Xorf19a1/2 using pKFAV4AP as the template, which was digested with SpeI/BstZ17I and used to replace the corresponding region in pKFAV4SAP-GFP to generate pKFAV4SAPX19a-GFP (pKFAV4SAP \times ORF19A GFP, 7119 bp) through restriction-ligation cloning. GFP was further replaced with mCherry gene in pKFAV4SAPX19a-GFP. Part of the CMV promoter (395 bp) was amplified with primers of 1904FAV4MCHE1/2 using pKFAV4-GFP as the template; mCherry CDS (733 bp) was amplified with primers of 1904FAV4MCHE3/4 using pmCherry-N1 (Clontech Laboratories, Mountain View, CA, USA) as the template; and these two PCR products were fused to generate a 1102 bp DNA fragment through overlap extension PCR. The PCR product was digested with NdeI/SalI and used to replace the corresponding region in pKFAV4SAPX19a-GFP to generate pKFAV7807-Che (7807 bp) through restriction-ligation cloning. pKFAV7807-Che was linearized with PacI and fused to the large fragment of SpeI/AvrII-digested pKFAV4M to generate pKFAV4-CX19A (pKFAV4 mCherry \times ORF19A, 43,528 bp) through DNA assembly.

2.7. Rescue, Amplification, Purification and Titration of Recombinant Virus

Adenoviral plasmid (pKFAV4-GFP, pKFAV4-GX4C or pKFAV4-CX19A) was linearized by PmeI-digestion, recovered by ethanol precipitation and used to transfect LMH cells after mixing with Lipofectamine 3000 reagents (Thermo Fisher Scientific, Waltham, MA, USA). Rescued viruses were amplified in LMH cells. Recombinant viruses were purified with standard CsCl discontinuous density gradient ultracentrifugation except that 10 mM citrate (pH6.2) instead of 10 mM Tris-Cl (pH7.6) was used as the buffer medium for preparing the CsCl solutions [13]. Adenoviral band was collected, dialyzed against a solution containing 10 mM sodium citrate, 150 mM sodium chloride and 5% glycerol (pH6.2), aliquoted and frozen at -80°C . Particle titer (viral particles per milliliter, vp/mL) of purified virus was determined by measuring the content of genomic DNA where 100 ng of genomic DNA is equivalent to 2.3×10^9 viral particles, since a 43-kb genome has a molecular mass of 2.6×10^7 . Infectious titer (infectious units per milliliter, IU/mL) was determined on LMH cells with the limiting dilution assay by counting GFP+ or mCherry+ cells two days after infection [15].

2.8. Identification of Recombinant Virus

Virus genomic DNA was extracted from virus-infected LMH cells using a modified Hirt's method [11,16]. Viral DNA was digested with restriction enzymes and resolved on 0.6% agarose gel containing ethidium bromide by electrophoresis. Primers were designed, synthesized and used for identification of viral genome by PCR (Table 1).

2.9. Plaque Forming Experiment

Exponentially growing LMH cells were seeded on 6-well plates. One day later, when cells reached 90% confluence, diluted viruses in 1.5 mL DMEM plus 2% FBS was added to each well. After two hours' inoculation, viruses were removed, and the cells were washed twice with 10 mM phosphate buffered saline (PBS) and covered with 2.5 mL DMEM containing 2% FBS and 0.7% low-melting agarose. Five days after infection, 2 mL fresh DMEM containing 2% FBS was supplemented to each well. At day 7 after infection, the liquid medium on the top was removed without damaging the semisolid overlay, and 2.5 mL 4% paraformaldehyde in PBS was added to each well. The cells were fixed at room temperature for 2 h, the semisolid medium was discarded, and cells were rinsed with running water before covering with 1.5 mL crystal violet solution for half an hour. After removing the staining solution, wells were rinsed with running water for several times and photographed [17]. The number of the plaques in each well was counted, and the area of each plaque was measured by using Fiji image processing package (<http://fiji.sc/>). The sizes of the plaques formed by different recombinant FAdV-4 were compared with the Kruskal–Wallis nonparametric test (GraphPad Prism 6).

2.10. Viral Inoculation of Embryonated Chicken Eggs

Specific pathogen free (SPF) chicken eggs were purchased from Beijing Boehringer Ingelheim Vital Biotechnology Company. Six day-old eggs were divided into four groups (15 eggs per group), inoculated with purified virus of 2×10^8 vp in 100 μ L PBS or only PBS via the yolk sac route, and cultured in a 37 °C incubator. The viability of the embryos was checked every 24 h. Livers from dead embryos were collected, weighed, smashed into small pieces, suspended in PBS and frozen in -80 °C. After three cycles of freeze-and-thaw, the liver suspension (six samples were selected from each virus-infected group) was spun at $1200 \times g$ for 5 min, and the supernatant was titrated on LMH cells with the limiting dilution method by counting fluorescence-positive cells. The yield of virus was normalized by the weight of the liver and presented as infectious units per gram of liver (IU/g). The study end point was set to the embryo age of 18 days, after that the viable embryos were killed by chilling the eggs at 4 °C overnight [18–20]. The data of embryonic lethality were subjected into survival analysis (GraphPad Prism 6).

3. Results

3.1. Reverse Genetics System for Modification of the Right End of FAdV-4 Genome

Schematic diagram of the establishment and application of the reverse genetics system was shown in Figure 1 and Figure S1. The fragment, which contained the right end of FAdV-4 genome, plasmid backbone and part of the left end of the viral genome, was separated from pKFAV4 by AvrII digestion and fused with artificially synthesized short DNA fragment, which contained the two overlaps for small plasmid assembly (OL-S1 and OL-S2), the two overlaps for large plasmid assembly (OL-L1 and OL-L2) and a PacI site, to generate the intermediate plasmid pKFAV4AP by DNA assembly. pKFAV4AP and pKFAV4 composed the reverse genetics system: the viral genes could be modified conveniently in pKFAV4AP, and the modified pKFAV4AP could be digested by PacI and restored to pKFAV4 by DNA assembly (Figure S1).

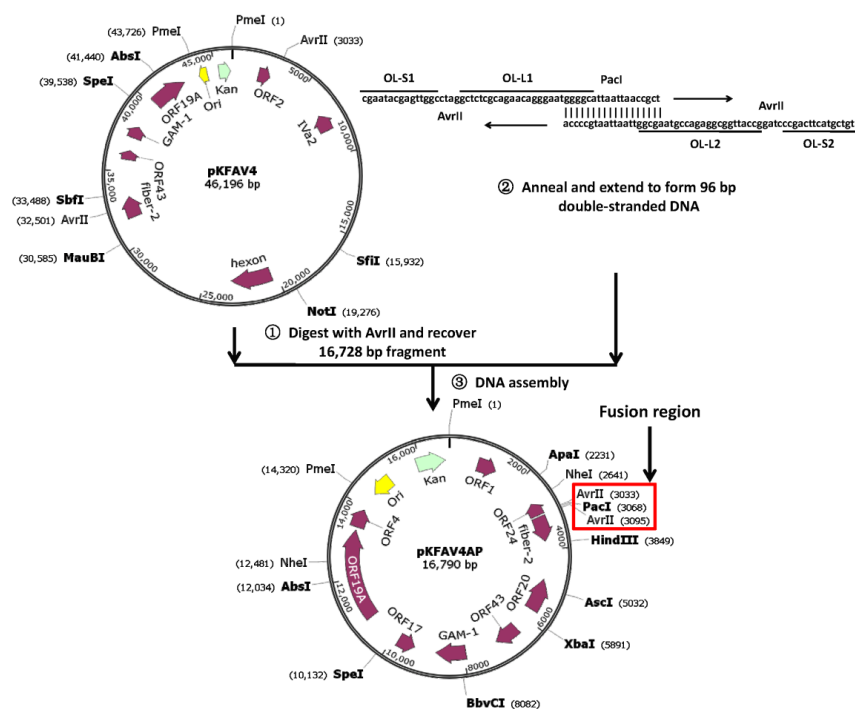


Figure 1. Schematic diagram for generating the intermediate plasmid pKFAV4AP (pKFAV4AvrII-PacI). The infectious clone pKFAV4 and pKFAV4AP composed a reverse genetics system for modification of the right end of fowl adenovirus 4 (FAdV-4): the gene mutation could be carried out in the small plasmid

pKFAV4AP, and the modified gene could be restored to the viral genome by DNA assembly. The unique restriction sites were labeled in bold, which could be used for gene modification through overlap extension PCR combined with restriction-ligation cloning. The fusion region, including the restriction sites, were highlighted in the red box. OL-S1 and OL-S2: overlaps for generating the small plasmid (intermediate plasmid) by DNA assembly; OL-L1 and OL-L2: overlaps for generating large plasmid (adenoviral plasmid) by DNA assembly.

3.2. Construction of Recombinant FAdV-4 with Deletions of ORF1, ORF1b and ORF2

DNA assembly was employed to fuse three fragments together to form a small plasmid pKFAV4APN-GFP, which contained the same sequence of the short fragment of NheI-digested pKFAV4AP except that the CDS of ORF1, ORF1b and ORF2 was replaced with the GFP expression cassette (Figure 2). pKFAV4APN-GFP was restored to pKFAV4AP by restriction-ligation, and the generated plasmid was further restored to pKFAV4 by DNA assembly to produce the adenoviral plasmid pKFAV4-GFP. GFP focuses appeared on LMH cells three days after being transfected with PmeI-linearized pKFAV4-GFP. These focuses grew and merged, and complete cytopathic effect (CPE) finally occurred five days after transfection, suggesting successful rescue of recombinant virus FAdV4-GFP (Figure 3A). The genomic DNA of FAdV4-GFP was extracted and identified by restriction analysis and PCR (Figure 3B,C). The results indicated that FAdV4-GFP was successfully constructed.

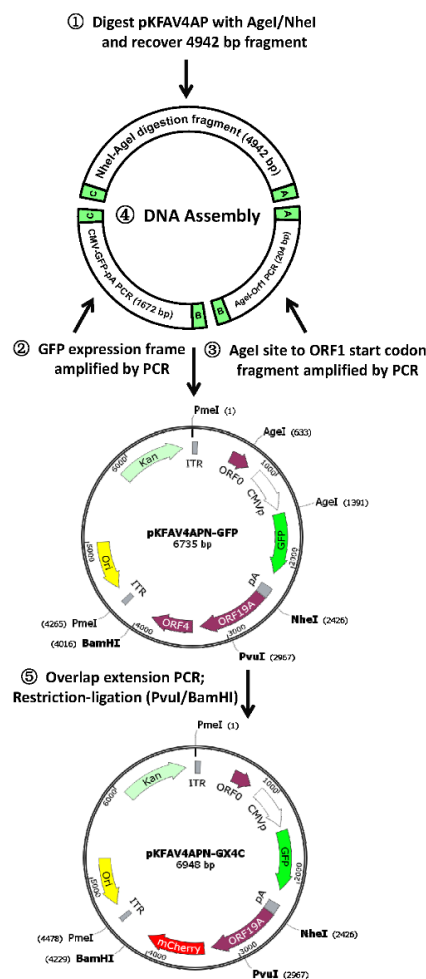


Figure 2. Schematic diagram for constructing small plasmid bearing fluorescent protein reporter genes. The DNA assembly of two PCR products and AgeI/NheI fragment in pKFAV4AP created plasmid pKFAV4APN-GFP (pKFAV4AP NheI-GFP), in which ORF1, ORF1b and ORF2 were replaced with Enhanced

Green Fluorescent Protein (GFP) expression cassette. The ORF4 coding sequence (CDS) was further replaced with that of mCherry to generate pKFAV4APN-GX4C (GFP-xORF4-mCherry). These two small plasmids were separately restored to pKFAV4AP by restriction-ligation cloning.

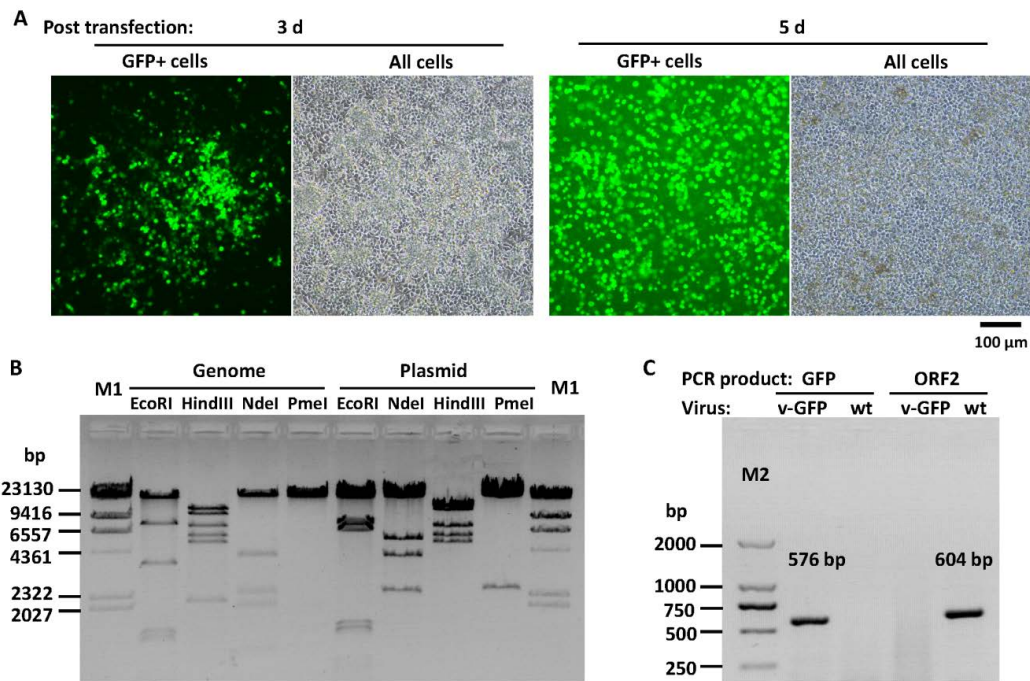


Figure 3. FAdV4-GFP rescue and identification. (A) Rescue of recombinant fowl adenovirus FAdV4-GFP. PmeI-linearized pKFAV4-GFP was used to transfect chicken hepatoma cells (Leghorn Male Hepatoma, LMH), and foci formed by GFP-positive cells could be observed under a fluorescence microscope three days after transfection. Growth and fusion of these foci led to cytopathic effect (CPE) five days after transfection. (B) Identification of FAdV4-GFP by restriction analysis of its genomic DNA with adenoviral plasmid pKFAV4-GFP as the control. The predicted molecular weights of digested fragments of the FAdV4-GFP genome were 463, 516, 699, 1248, 1384, 3584, 7836 and 27,774 bp for EcoRI; 2151, 5216, 5900, 7413, 10,468 and 12,356 bp for HindIII; 251, 1016, 1975, 2352, 3993 and 33,917 bp for NdeI; and PmeI did not cut. The predicted molecular weights of digested fragments of pKFAV4-GFP plasmid were 463, 699, 1248, 1384, 6577, 7836 and 27,774 bp for EcoRI; 5216, 5900, 7413, 12,356 and 15,096 bp for HindIII; 251, 2352, 3993, 5468 and 33,917 bp for NdeI; and 2471 and 43,510 bp for PmeI. (C) Identification of FAdV4-GFP by PCR. PCR was performed to amplify fragments inside GFP or ORF2 genes using the FAdV4-GFP genomic DNA (v-GFP) as the template, and the products were resolved on 1% agarose gel. Wild-type FAdV-4 genome (wt) served as a control template. The results indicated that FAdV4-GFP was successfully constructed.

3.3. Construction of Recombinant FAdV-4 with Deletions of ORF1, ORF1b, ORF2 and ORF4

ORF4 is a viral gene located at the very right end of the genome. The CDS of ORF4 in pKFAV4APN-GFP was replaced with that of mCherry through overlap extension PCR-mediated site-directed mutation (Figure 2). The generated pKFAV4APN-GX4C (GFP-xORF4-mCherry) plasmid, in which ORF1, ORF1b, ORF2 and ORF4 were deleted, was restored to pKFAV4 to form pKFAV4-GX4C with the same procedure of constructing pKFAV4-GFP. Recombinant FAdV4-GX4C was rescued similarly. Because it carried both GFP and mCherry genes, the foci showed green and red fluorescence when observed under fluorescence microscope (Figure 4A). The genomic DNA was further identified by restriction analysis and PCR (Figure 4B,C). The results demonstrated that FAdV4-GX4C was correctly generated.

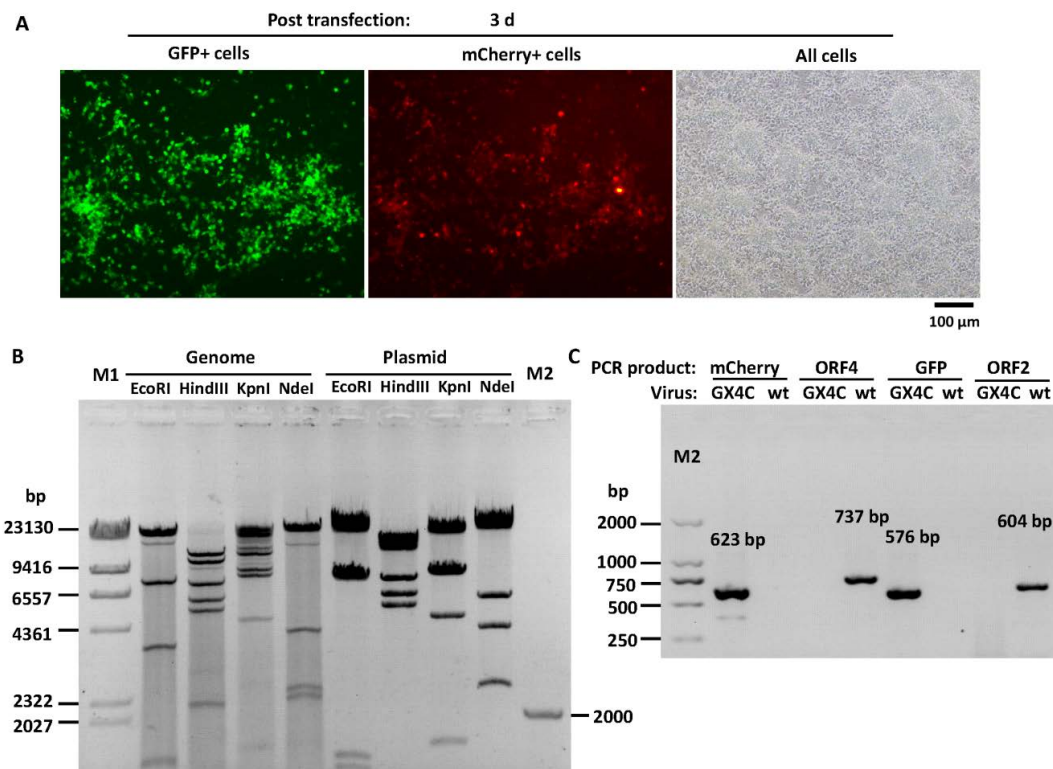


Figure 4. FAdV4-GX4C rescue and identification. (A) Rescue of recombinant fowl adenovirus FAdV4-GX4C. PmeI-linearized pKFAV4-GX4C was used to transfect LMH cells, and focuses formed by GFP- and mCherry-positive cells could be observed under a fluorescence microscope three days after transfection. (B) Identification of FAdV4-GX4C by restriction analysis of its genomic DNA with adenoviral plasmid pKFAV4-GX4C as the control. The predicted molecular weights of digested fragments of the FAdV4-GX4C genome were 463, 1248, 1384, 1428, 3584, 7836 and 27,774 bp for EcoRI; 2151, 5216, 5900, 7413, 10,681 and 12,356 bp for HindIII; 935, 1542, 4546, 7990, 8123, 8840 and 11,741 bp for KpnI; and 251, 1016, 2188, 2352, 3993 and 33,917 bp for NdeI. The predicted molecular weights of digested fragments of pKFAV4-GX4C plasmid were 463, 1248, 1384, 7489, 7836 and 27,774 bp for EcoRI; 5216, 5900, 7413, 12,356 and 15,309 bp for HindIII; 935, 1542, 4546, 7990, 8123 and 23,058 bp for KpnI; and 251, 2352, 3993, 5681 and 33,917 bp for NdeI. (C) Identification of FAdV4-GX4C by PCR. PCR was performed to amplify fragments inside mCherry, ORF4, GFP or ORF2 genes using the FAdV4-GX4C genomic DNA (GX4C) as the template, and the products were resolved on 1% agarose gel. Wild-type FAdV-4 genome (wt) served as a control template.

3.4. Modification of the Reverse Genetics Systems

On the map of the intermediate plasmid pKFAV4AP, it could be learned that it contained unique restriction sites of ApaI, PacI, HindIII, AscI, XbaI, BbvCI, SpeI and AbsI (Figure 1). Therefore, gene sequence among these restriction sites could be easily modified through one step of overlap extension PCR-mediated site-directed mutation. However, it spans 7 kb from AbsI to ApaI sites in the clockwise direction. There is no typical unique restriction site that can be used in the middle of this region, which makes modification of genes in this region more difficult. That is why a smaller plasmid pKFAV4APN-GFP was constructed and two steps of restoration were needed for generation of pKFAV4-GFP and pKFAV4-GX4C. To simplify the procedure, The AvrII site inside the fiber-2 gene was removed without change of the amino acid it encoded to generate a mutant pKFAV4 (pKFAV4M; Figure S2); and a smaller intermediate plasmid pKFAV4SAP-GFP was also constructed (Figure S3). pKFAV4SAP-GFP and pKFAV4M composed the modified reverse genetics system, which could be used to modify the regions upstream of the AvrII site at the left and downstream of the SpeI site at the right in the FAdV-4 genome (Figure S2).

3.5. Construction of Recombinant FAdV-4 with Deletion of ORF1, ORF1b, ORF2 and ORF19A

The modified system was validated by deletion of ORF19A. Overlap extension PCR-mediated site-directed mutations were carried out to delete the ORF19A CDS and replace the GFP with mCherry in pKFAV4SAP-GFP (Figure S3). The generated plasmid pKFAV7087-Che was linearized by *PacI* digestion and fused with the large fragment of *SpeI*/*AvrII* digested pKFAV4M to generate pKFAV4-CX19A (mCherry-xORF19A, Figure S3). Recombinant virus was rescued from LMH cells transfected with *PmeI*-linearized pKFAV4-CX19A. The viral genome (FAdV4-CX19A) was further identified by restriction analysis and PCR (Figure 5A,B). The results indicated that FAdV4-CX19A was correctly constructed.

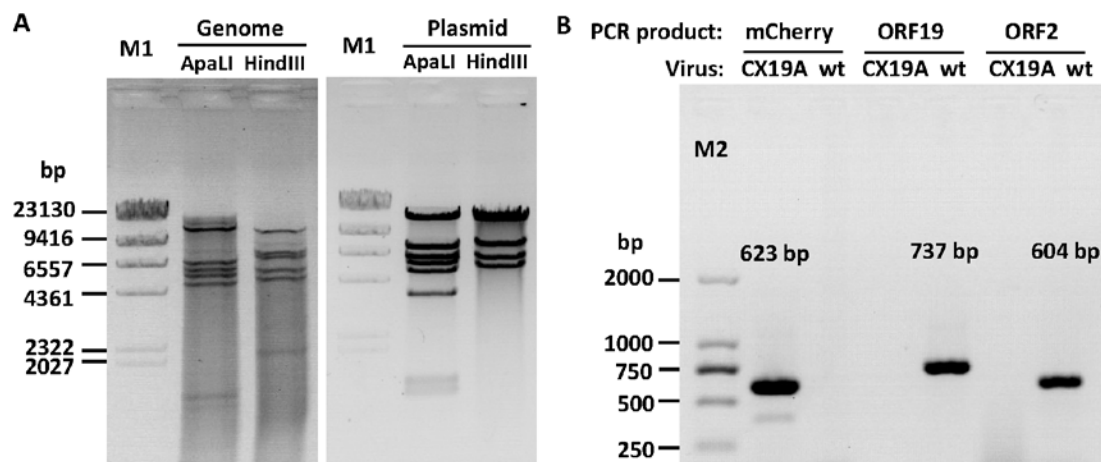


Figure 5. Identification of FAdV4-CX19A virus. (A) FAdV4-CX19A (mCherry-xORF19A) was identified by restriction analysis of its genomic DNA, and adenoviral plasmid pKFAV4-CX19A served as the control. The predicted molecular weights of digested fragments of the FAdV4-CX19A genome were 1312, 1447, 1450, 4879, 5592, 6113, 6904 and 13,354 bp for *Apa*LI; and 2119, 5216, 5900, 7413, 8047 and 12,356 bp for *Hind*III. The predicted molecular weights of digested fragments of pKFAV4-CX19A plasmid 1312, 1450, 3527, 4879, 5592, 6113, 7301 and 13,354 bp for *Apa*LI; and 5216, 5900, 7413, 12,356 and 12,643 bp for *Hind*III. (B) Identification of FAdV4-CX19A by PCR. PCR was performed to amplify fragments inside mCherry, ORF19A or ORF2 genes using the FAdV4-CX19A genomic DNA (CX19A) as the template, and the products were resolved on 1% agarose gel. Wild-type FAdV-4 genome (wt) served as the control template.

3.6. Growth Property of Recombinant Viruses in LMH Cells

The purified recombinant FAdV-4 viruses had a physical particle-to-infectious unit (IU) ratio of 200 to 300. LMH cells in 12-well plate were infected with purified viruses at a multiplicity of infection (MOI) of 50 vp/cell for 2 h, and the progeny viruses were harvested 48 or 72 h after infection and titrated on LMH cells. It could be seen that the FAdV4-CX19A had the highest replication ability, followed by FAdV4-GFP and FAdV4-GX4C in sequence (Figure 6A). The difference in viral replication in vitro was confirmed by plaque forming assay (Figure 6B). FAdV4-CX19A formed the largest plaques on LMH confluent monolayer cells while FAdV4-GX4C formed the smallest (Figure 6B,C). There was no significant difference in plaque numbers between the three recombinant viruses when the same amount viruses were used to infect LMH cells on six-well plates. One-step growth curve assay was further conducted to compare growth property of FAdV-4 and recombinant viruses (Figure S4). While FAdV-4 and FAdV4-GFP had similar growth characteristic in LMH cells, the replication rates successively increased among FAdV4-GX4C, FAdV4-GFP and FAdV4-CX19A. The results indicated that deletion of ORF4 or ORF19A altered the replication ability of FAdV-4.

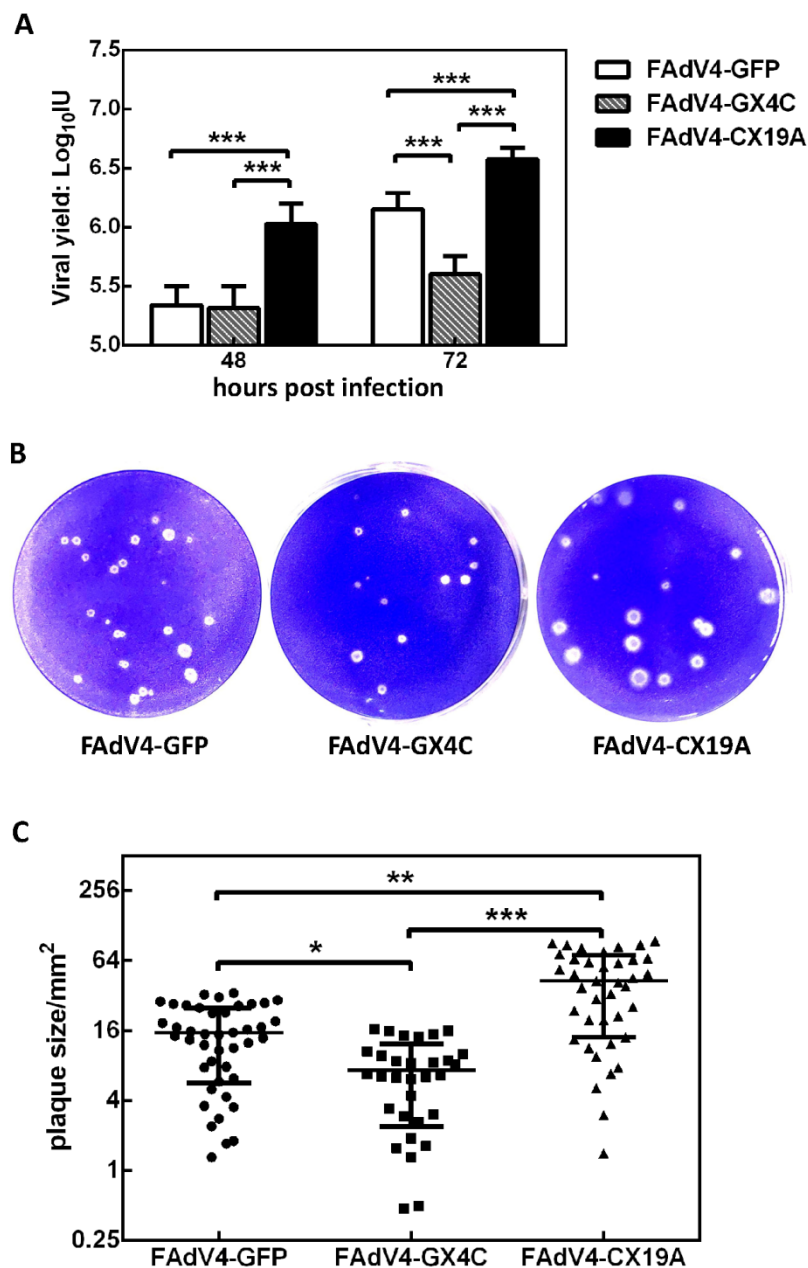


Figure 6. Viral replication in LMH cells. (A) LMH cells in 12-well plates were infected with FAdV4-GFP, FAdV4-GX4C or FAdV4-CX19A at a multiplicity of infection (MOI) of 50 vp/cell for 2 h. The progeny viruses were harvested 48 or 72 h after infection, and titrated on LMH cells. The viral yield (infectious units, IU) in one well was calculated and shown. (B) LMH cells in 6-well plates were infected with FAdV4-GFP, FAdV4-GX4C or FAdV4-CX19A at an amount of 8000 vp/well for 2 h. Cells were covered with semi-solid culture medium and cultivated for seven days before fixing and staining to show the plaques. (C) The area of each plaque was measured with the help of Fiji image processing package. The data from the three viruses were collected and analyzed with the Kruskal–Wallis nonparametric test. * $p < 0.05$, ** $p < 0.01$, and *** $p < 0.001$.

3.7. Expression of mCherry Controlled by the FAdV-4 ORF4 Promoter in LMH Cells

In order to evaluate the possibility of expressing exogenous gene with FAdV-4 ORF4 original promoter, the coding sequence of ORF4 was replaced with that of mCherry reporter gene in FAdV4-GFP to generate FAdV4-GX4C. The expression of GFP or mCherry under CMV promoter in FAdV4-GX4C or FAdV4-CX19A served as controls. No expression of mCherry could be observed in

FAdV4-GX4C-infected LMH cells 9 h after infection while the expression of GFP could be seen clearly in the same culture. The fluorescence of mCherry became obvious in FAdV4-GX4C-infected LMH cells 24 h after infection although it was still substantially weaker than GFP in the same cells or mCherry in FAdV4-CX19A-infected cells. At 48 h after infection, the expression of mCherry increased slightly in FAdV4-GX4C-infected LMH when the viruses started to lyse the cells and the released GFP in FAdV4-GX4C-infected and mCherry in FAdV4-CX19A-infected cultures could be seen in the media (Figure 7). The results suggested that ORF4 was a non-essential gene and the promoter of ORF4 could be employed to express exogenous gene although it was weak.

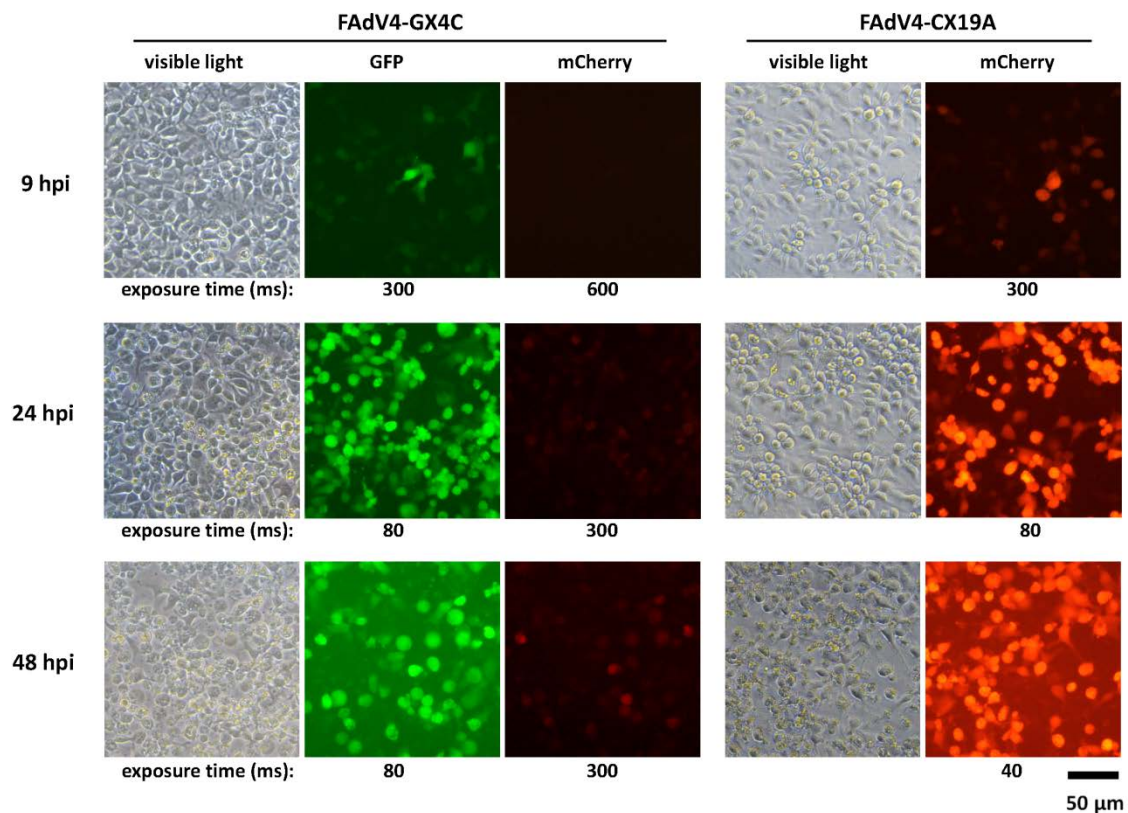


Figure 7. Expression of mCherry under the ORF4 promoter of FAdV-4. LMH cells were infected with FAdV4-GX4C and FAdV-CX19A. The expression of GFP and mCherry was observed under fluorescence microscope at 9, 24 and 48 h after infection (hpi). In FAdV4-GX4C, GFP was controlled by the CMV promoter while mCherry was controlled by the ORF4 original promoter. In FAdV4-CX19A, mCherry was controlled by the CMV promoter. The results indicated that the ORF4 original promoter was a weak one in LMH cells.

3.8. Embryonic Lethality of Recombinant FAdV-4 Infection in Chicken

Embryonated eggs could be used as an experimental alternative to chickens to preliminarily evaluate the mortality of virus infection. The virulence of FAdV4-GFP, -GX4C and -CX19A was compared by inoculating embryonated chicken eggs via yolk sac route. The death of embryos inoculated with FAdV4-GX4C started from day 5 and ended at day 10 after infection with a mortality of 100%. FAdV4-GFP inoculation caused the embryos to die from day 8 after infection, and all infected embryos died within two days. The survival curve of FAdV4-CX19A-infected embryos shifted rightward by nearly one day when compared with that of FAdV4-GFP inoculation (Figure 8A). The results of survival analysis showed that the survival curve of FAdV4-CX19A was significantly different from that of FAdV4-GFP while the difference between FAdV4-GX4C and FAdV4-GFP was not statistically significant. All viruses could be recovered from the livers of dead embryos. It seemed that there was an enhanced replication of FAdV4-CX19A in chicken embryos when compared with that of

the other two viruses although the difference was not significant (Figure 8B). Embryonated eggs were used to propagate FAdV-4 in the laboratory previously, and it could be deduced that FAdV4-GFP had similar embryonic lethality with FAdV-4 [13]. The results suggested that ORF19A was related to the virulence of FAdV-4 although it was nonessential for virus replication. Because the immune system of chicken embryo is in development and is different from that of newly hatched or adult birds [21], the effect of ORF19A deletion on FAdV-4 virulence in chickens deserves further study.

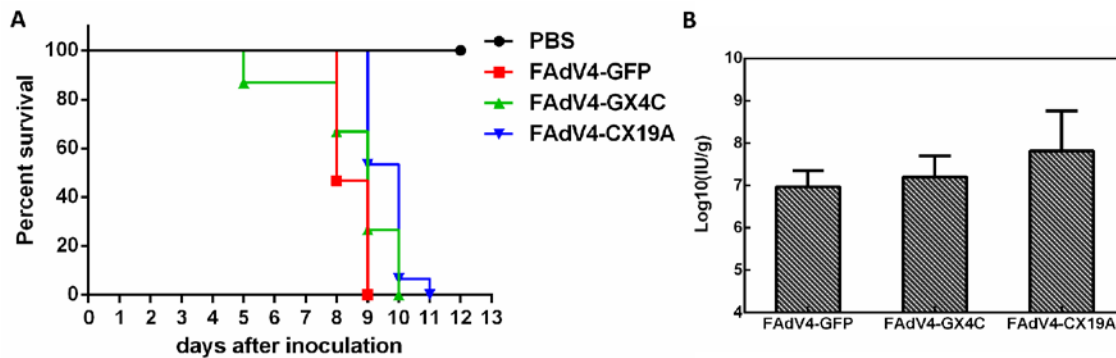


Figure 8. Inoculation of embryonated chicken eggs with recombinant FAdV-4. Sixty six-day old embryonated chicken eggs were randomly divided into four groups (15 eggs per group), and three groups were inoculated with FAdV4-GFP, FAdV4-GX4C or FAdV4-CX19A of 2×10^8 vp in 100 μ L PBS via yolk sac route, respectively. The PBS group was injected with 100 μ L PBS containing no virus, and served as uninfected control. The viability of embryos was checked every 24 h. Livers from dead embryos were weighed and collected for virus titration. (A) Survival curve of embryonated chicken eggs after viral inoculation. (B) Virus amount in liver normalized by liver weight, which was shown as infectious units per gram of liver (IU/g).

4. Discussion

The genus-specific genes of FAdV have no similarity to those of HAdV. The function of FAdV genus-specific genes has not been investigated, except for ORF1 (dUTPase), ORF8 (Gam-1) and ORF22 [22,23]. It has priorities to study the functions of FAdV genus-specific genes. These genes are engaged in the interaction between FAdV and the host cell or host immune system [2,8]. Elucidation of the gene functions will facilitate the development of attenuated vaccines, which have the advantages over inactivated or subunit vaccines of high efficacy, easy inoculation and low costs [24–27]. On the other hand, gene function study will help the construction of FAdV-based gene delivery tools. FAdV vectors can well complement the use of those based on mammalian adenoviruses. For instance, FAdV vectors can be used to construct vector vaccines against other infectious diseases of fowl, or to take the place of HAdV in human gene therapies in situation the effect of HAdV vectors will be compromised because of the neutralizing antibodies. Other possible advantages of FAdV vectors include higher cloning capacity, more stable physicochemical properties and lower cost in vector production [28]. A user-friendly reverse genetics system may help expedite FAdV gene function study.

The FAdV vectors were constructed with the strategy of bacterial homologous recombination two decades ago [28]. This platform was further modified and improved by Eva Nagy and her colleagues through introducing phage recombinase [10]. Recently, CRISPR/Cas9 was employed as a tool to introduce double-stranded breaks at targeting site in FAdV genome to increase the percentage of positive recombinants in eukaryotic cells [29]. The homologous recombination in bacteria with phage recombinase and counter-selection technique were combined and used for modifying the FAdV-4 genome [30]. All these methods utilized the activity of recombinase inside cells.

Instead of eukaryotic or prokaryotic systems of homologous recombination, we employed the strategy of combining restriction enzyme digestion and isothermal DNA assembly for site-directed modification of FAdV-4 here, which were absolutely cell-free reaction systems [31,32]. The schematic diagram of our strategy, which we call restriction-assembly for convenience's sake, was shown

in Figure S1. A short fragment, in which the region for future modification locates, is excised from the plasmid of infectious clone by a dual cutter restriction enzyme; an intermediate plasmid is generated through two-fragment Gibson assembly; site-directed mutation is carried out in the intermediate plasmid with traditional methods such as overlap extension PCR; and finally the modified intermediate plasmid is linearized by restriction digestion and restored to the adenoviral genome through two-fragment DNA assembly. The approximately 100-bp long DNA fragment, which includes sequences flanking the dual cutter sites in the adenoviral genome and one extra restriction enzyme site for the future linearization of the modified intermediate plasmid, does the job of the left and right homolog arms in homologous recombination and mediates the generation of intermediate plasmid and future modified adenoviral plasmid. The restriction-assembly strategy is different from homologous recombination strategy in following aspects [33]. The presence of recombinase and identical sequences triggers homologous recombination, which could also be a cause for the instability of plasmids in which identical or repeat regions exist. In contrast, DNA exonuclease, polymerase and ligase are included in Gibson assembly [31], which ensures the assembly reactions proceed only between the short overlaps at the ends of but not inside DNA fragments; and recombinase-negative bacteria are generally chosen as the host cells for following plasmid transformation and propagation, which is good for keeping plasmids stable. Homologous recombination requires longer homolog arms than DNA assembly. Homolog arms about 50-bp in length are needed for bacteriophage recombinase-mediated recombination, while efficient recombination in *Escherichia coli* BJ5183 strain demands identical sequences as long as hundreds of base pairs. DNA assembly can take place between overlaps as short as 15 bp if the value of the melting temperature (T_m) is more than 48 °C. In addition, generic materials such as restriction enzymes, chemically competent *Escherichia coli* cells, PCR reagents and DNA assembly kit can satisfy the whole procedure of restriction-assembly in labs of molecular biology. For the homologous recombination strategy, bacterial strains expressing recombinase and electroporation are often indispensable [34]. All these facts claim the advantages of restriction-assembly strategy.

The whole genomes of FAdV were thoroughly analyzed with methods of biological informatics although only three genus-specific genes have been studied so far [2,8,23]. It was reported that ORFs 0, 1, 1A,1B, 1C and 2 at the left and TR-2, ORFs 11, 17 and 19 at the right of the genome were nonessential genes for FAdV-9, and ORFs 16 and 17 were dispensable for FAdV-4 [10,22]. Here, we found that ORF1, ORF1b and ORF2 at the left end of the genome were nonessential for FAdV-4 replication. FAdV-C, in which species FAdV-4 and -10 are included, has species-specific genes of ORF4 and ORF19A at the rightmost end of the genome. ORF4 and ORF19A can only be found in FAdV-C. Therefore, it is conceivable that they might be responsible for HHS caused by FAdV-4. However, whether these species-specific genes contribute to the virulence of the novel FAdV-4 remains unknown.

FAdV-4 ORF4 is a US22 protein [2]. US22 family was first described in human cytomegalovirus (HCMV), members of which are clustered at the end of HCMV genome [35,36]. US22 proteins are found in all betaherpesviruses and some animal viruses such as gallid alphaherpesvirus, fowlpox virus and iridovirus [37]. US22 family is predicted to counter anti-viral responses by interacting with specific host proteins although little is known about the detailed functions [37,38]. Our results showed that the ORF4 was non-essential for viral replication in LMH cells or in chicken embryos. However, it played roles in viral propagation since ORF4-deleted virus formed smaller plaques (Figure 6). Deletion of ORF4 could not prolong the survival of virus-infected chicken embryos. The CDS replacement experiments suggested that the promoter of ORF4 might be a weak one in LMH cells considering low level expression of mCherry in FAdV4-GX4C infected LMH cells (Figure 7).

FAdV ORF19 encodes a polypeptide with predicted lipase function. Most FAdVs have one ORF19 gene while FAdV-C contains a duplicate homolog ORF19A besides ORF19. To make things more intriguing, the highly pathogenic FAdV-4 loses ORF19 due to a 1966 bp deletion. However, it has been reported that the deletion of ORF19 does not contribute to the viral virulence [29,30]. We are interested in whether the remaining unique ORF19A influences the replication of the novel FAdV-4. Deletion of ORF19A enhanced viral propagation in LMH cells (Figure 6). A slight increase of viral yield in liver

could also be observed in FAdV4-CX19A-infected chicken embryos. However, deletion of ORF19A in FAdV-4 made the embryos survive one more day when compared with those infected by FAdV4-GFP, an ORF19A-intact control (Figure 8), suggesting ORF19A participates in FAdV-4 pathogenesis. Whether and how the deletion of ORF19A reduces FAdV-4 virulence in chicken deserves further study, which may provide clues for developing attenuated vaccines against the novel FAdV-4 infection.

In summary, we established a reverse genetics system to facilitate modification of the right end of the highly pathogenic FAdV-4 genome. We found the species-specific genes of ORF4 and ORF19A were dispensable for the growth of FAdV-4 although they influenced viral replication or virulence. This work will benefit the study of FAdV-4 gene function and vaccine development.

Supplementary Materials: Supplementary materials can be found at <http://www.mdpi.com/1999-4915/12/3/301/s1>.

Author Contributions: Conceptualization, Z.L. and Y.L.; methodology, Z.L., B.Y. and X.Z.; validation, X.G. and X.L.; investigation, B.Y., X.Z., X.L., J.Z. and W.Z.; resources, Z.L.; writing—original draft preparation, Z.L. and X.Z.; writing—review and editing, Z.L.; visualization, B.Y., X.Z. and Z.L.; supervision, Z.L. and Y.L.; project administration, M.W.; funding acquisition, X.Z. and Z.L. All authors have read and agreed to the published version of the manuscript.

Funding: This work was supported by National Science and Technology Major Projects (No. 2018ZX10305-410-003-002 and 2018ZX10734404).

Conflicts of Interest: The authors declare no conflict of interest. The funders had no role in the design of the study; in the collection, analyses, or interpretation of data; in the writing of the manuscript, or in the decision to publish the results.

References

1. King, A.M.Q.; Adams, M.J.; Carstens, E.B.; Lefkowitz, E.J. *Virus taxonomy: Classification and nomenclature of viruses: Ninth Report of the International Committee on Taxonomy of Viruses*; Elsevier Academic Press: San Diego, CA, USA, 2011; pp. 129–141.
2. Corredor, J.C.; Garceac, A.; Krell, P.J.; Nagy, E. Sequence comparison of the right end of fowl adenovirus genomes. *Virus Genes* **2008**, *36*, 331–344. [[CrossRef](#)]
3. Schachner, A.; Matos, M.; Graf, B.; Hess, M. Fowl adenovirus-induced diseases and strategies for their control—a review on the current global situation. *Avian Pathol.* **2018**, *47*, 111–126. [[CrossRef](#)] [[PubMed](#)]
4. Anjum, A.D.; Sabri, M.A.; Iqbal, Z. Hydropericarditis syndrome in broiler chickens in Pakistan. *Vet. Rec* **1989**, *124*, 247–248. [[CrossRef](#)] [[PubMed](#)]
5. Chen, L.; Yin, L.; Zhou, Q.; Peng, P.; Du, Y.; Liu, L.; Zhang, Y.; Xue, C.; Cao, Y. Epidemiological investigation of fowl adenovirus infections in poultry in China during 2015–2018. *BMC Vet. Res.* **2019**, *15*, 271. [[CrossRef](#)] [[PubMed](#)]
6. Li, P.H.; Zheng, P.P.; Zhang, T.F.; Wen, G.Y.; Shao, H.B.; Luo, Q.P. Fowl adenovirus serotype 4: Epidemiology, pathogenesis, diagnostic detection, and vaccine strategies. *Poult. Sci.* **2017**, *96*, 2630–2640. [[CrossRef](#)]
7. Liu, Y.; Wan, W.; Gao, D.; Li, Y.; Yang, X.; Liu, H.; Yao, H.; Chen, L.; Wang, C.; Zhao, J. Genetic characterization of novel fowl aviadenovirus 4 isolates from outbreaks of hepatitis-hydropericardium syndrome in broiler chickens in China. *Emerg. Microbes. Infect.* **2016**, *5*, e117. [[CrossRef](#)]
8. Davison, A.J.; Benko, M.; Harrach, B. Genetic content and evolution of adenoviruses. *J. Gen. Virol.* **2003**, *84*, 2895–2908. [[CrossRef](#)]
9. Sheppard, M.; Werner, W.; Tsatas, E.; McCoy, R.; Prowse, S.; Johnson, M. Fowl adenovirus recombinant expressing VP2 of infectious bursal disease virus induces protective immunity against bursal disease. *Arch. Virol.* **1998**, *143*, 915–930. [[CrossRef](#)]
10. Corredor, J.C.; Pei, Y.; Nagy, E. Fowl Adenovirus-Based Vaccine Platform. *Methods Mol. Biol.* **2017**, *1581*, 29–54. [[CrossRef](#)]
11. Liu, H.; Lu, Z.; Zhang, X.; Guo, X.; Mei, L.; Zou, X.; Zhong, Y.; Wang, M.; Hung, T. Single Plasmid-Based, Upgradable, and Backward-Compatible Adenoviral Vector Systems. *Hum. Gene. Ther.* **2019**. [[CrossRef](#)]
12. Guo, X.; Mei, L.; Yan, B.; Zou, X.; Hung, T.; Lu, Z. Site-directed modification of adenoviral vector with combined DNA assembly and restriction-ligation cloning. *J. Biotechnol.* **2019**, *307*, 193–201. [[CrossRef](#)] [[PubMed](#)]

13. Zou, X.H.; Bi, Z.X.; Guo, X.J.; Zhang, Z.; Zhao, Y.; Wang, M.; Zhu, Y.L.; Jie, H.Y.; Yu, Y.; Hung, T.; et al. DNA assembly technique simplifies the construction of infectious clone of fowl adenovirus. *J. Virol. Methods* **2018**, *257*, 85–92. [[CrossRef](#)] [[PubMed](#)]
14. Lu, Z.Z.; Zou, X.H.; Dong, L.X.; Qu, J.G.; Song, J.D.; Wang, M.; Guo, L.; Hung, T. Novel recombinant adenovirus type 41 vector and its biological properties. *J. Gene Med.* **2009**, *11*, 128–138. [[CrossRef](#)] [[PubMed](#)]
15. Chen, D.L.; Dong, L.X.; Li, M.; Guo, X.J.; Wang, M.; Liu, X.F.; Lu, Z.Z.; Hung, T. Construction of an infectious clone of human adenovirus type 41. *Arch. Virol.* **2012**, *157*, 1313–1321. [[CrossRef](#)]
16. Arad, U. Modified Hirt procedure for rapid purification of extrachromosomal DNA from mammalian cells. *Biotechniques* **1998**, *24*, 760–762. [[CrossRef](#)]
17. Baer, A.; Kehn-Hall, K. Viral concentration determination through plaque assays: Using traditional and novel overlay systems. *J. Vis. Exp.* **2014**. [[CrossRef](#)]
18. Brauer, R.; Chen, P. Influenza virus propagation in embryonated chicken eggs. *J. Vis. Exp.* **2015**. [[CrossRef](#)]
19. Alemnesh, W.; Hair-Bejo, M.; Aini, I.; Omar, A.R. Pathogenicity of fowl adenovirus in specific pathogen free chicken embryos. *J. Comp. Pathol.* **2012**, *146*, 223–229. [[CrossRef](#)]
20. Cowen, B.S. Chicken embryo propagation of type I avian adenoviruses. *Avian Dis.* **1988**, *32*, 347–352. [[CrossRef](#)]
21. Abdul-Cader, M.S.; Palomino-Tapia, V.; Amarasinghe, A.; Ahmed-Hassan, H.; De Silva Senapathi, U.; Abdul-Careem, M.F. Hatchery Vaccination Against Poultry Viral Diseases: Potential Mechanisms and Limitations. *Viral Immunol.* **2018**, *31*, 23–33. [[CrossRef](#)]
22. Pei, Y.; Corredor, J.C.; Krell, P.J.; Nagy, E. Fowl adenovirus 9 ORF19, a lipase homolog, is nonessential for virus replication and is suitable for foreign gene expression. *Virus Res.* **2019**, *260*, 129–134. [[CrossRef](#)] [[PubMed](#)]
23. Griffin, B.D.; Nagy, E. Coding potential and transcript analysis of fowl adenovirus 4: Insight into upstream ORFs as common sequence features in adenoviral transcripts. *J. Gen. Virol.* **2011**, *92*, 1260–1272. [[CrossRef](#)] [[PubMed](#)]
24. Wang, X.; Tang, Q.; Qiu, L.; Yang, Z. Penton-dodecahedron of fowl adenovirus serotype 4 as a vaccine candidate for the control of related diseases. *Vaccine* **2019**, *37*, 839–847. [[CrossRef](#)] [[PubMed](#)]
25. Ruan, S.; Zhao, J.; Yin, X.; He, Z.; Zhang, G. A subunit vaccine based on fiber-2 protein provides full protection against fowl adenovirus serotype 4 and induces quicker and stronger immune responses than an inactivated oil-emulsion vaccine. *Infect. Genet. Evol.* **2018**, *61*, 145–150. [[CrossRef](#)]
26. Chen, L.; Yin, L.; Zhou, Q.; Li, Q.; Luo, Y.; Xu, Z.; Zhang, Y.; Xue, C.; Cao, Y. Immunogenicity and protective efficacy of recombinant fiber-2 protein in protecting SPF chickens against fowl adenovirus 4. *Vaccine* **2018**, *36*, 1203–1208. [[CrossRef](#)]
27. Grgic, H.; Poljak, Z.; Sharif, S.; Nagy, E. Pathogenicity and cytokine gene expression pattern of a serotype 4 fowl adenovirus isolate. *PLoS ONE* **2013**, *8*, e77601. [[CrossRef](#)]
28. Michou, A.I.; Lehrmann, H.; Saltik, M.; Cotten, M. Mutational analysis of the avian adenovirus CELO, which provides a basis for gene delivery vectors. *J. Virol.* **1999**, *73*, 1399–1410. [[CrossRef](#)]
29. Pan, Q.; Wang, J.; Gao, Y.; Cui, H.; Liu, C.; Qi, X.; Zhang, Y.; Wang, Y.; Wang, X. The Natural Large Genomic Deletion Is Unrelated to the Increased Virulence of the Novel Genotype Fowl Adenovirus 4 Recently Emerged in China. *Viruses* **2018**, *10*, 494. [[CrossRef](#)]
30. Zhang, Y.; Liu, R.; Tian, K.; Wang, Z.; Yang, X.; Gao, D.; Zhang, Y.; Fu, J.; Wang, H.; Zhao, J. Fiber2 and hexon genes are closely associated with the virulence of the emerging and highly pathogenic fowl adenovirus 4. *Emerg. Microbes Infect.* **2018**, *7*, 199. [[CrossRef](#)]
31. Gibson, D.G.; Young, L.; Chuang, R.Y.; Venter, J.C.; Hutchison, C.A., 3rd; Smith, H.O. Enzymatic assembly of DNA molecules up to several hundred kilobases. *Nat. Methods* **2009**, *6*, 343–345. [[CrossRef](#)]
32. Yonemoto, I.T.; Weyman, P.D. Facile Site-Directed Mutagenesis of Large Constructs Using Gibson Isothermal DNA Assembly. *Methods Mol. Biol.* **2017**, *1498*, 359–366. [[CrossRef](#)]
33. Lee, C.S.; Bishop, E.S.; Zhang, R.; Yu, X.; Farina, E.M.; Yan, S.; Zhao, C.; Zheng, Z.; Shu, Y.; Wu, X.; et al. Adenovirus-Mediated Gene Delivery: Potential Applications for Gene and Cell-Based Therapies in the New Era of Personalized Medicine. *Genes Dis.* **2017**, *4*, 43–63. [[CrossRef](#)]
34. Mizuguchi, H.; Kay, M.A.; Hayakawa, T. Approaches for generating recombinant adenovirus vectors. *Adv. Drug Deliv. Rev.* **2001**, *52*, 165–176. [[CrossRef](#)]

35. Chee, M.S.; Bankier, A.T.; Beck, S.; Bohni, R.; Brown, C.M.; Cerny, R.; Horsnell, T.; Hutchison, C.A., 3rd; Kouzarides, T.; Martignetti, J.A.; et al. Analysis of the protein-coding content of the sequence of human cytomegalovirus strain AD169. *Curr. Top. Microbiol. Immunol.* **1990**, *154*, 125–169. [[CrossRef](#)] [[PubMed](#)]
36. Menard, C.; Wagner, M.; Ruzsics, Z.; Holak, K.; Brune, W.; Campbell, A.E.; Koszinowski, U.H. Role of murine cytomegalovirus US22 gene family members in replication in macrophages. *J. Virol.* **2003**, *77*, 5557–5570. [[CrossRef](#)]
37. Zhang, D.; Iyer, L.M.; Aravind, L. A novel immunity system for bacterial nucleic acid degrading toxins and its recruitment in various eukaryotic and DNA viral systems. *Nucleic Acids Res.* **2011**, *39*, 4532–4552. [[CrossRef](#)]
38. Zmasek, C.M.; Knipe, D.M.; Pellett, P.E.; Scheuermann, R.H. Classification of human Herpesviridae proteins using Domain-architecture Aware Inference of Orthologs (DAIO). *Virology* **2019**, *529*, 29–42. [[CrossRef](#)]



© 2020 by the authors. Licensee MDPI, Basel, Switzerland. This article is an open access article distributed under the terms and conditions of the Creative Commons Attribution (CC BY) license (<http://creativecommons.org/licenses/by/4.0/>).